



WP1 report for
FRESCO+ version 2 for GOME-2 Metop-C processing

(short title: “FRESCO+ v2 for Metop-C”)

Ping Wang, Olaf Tuinder, Piet Stammes



Table of Contents

1 Introduction.....	4
2 FRESCO+ v2 LUT for GOME-2C.....	4
3 Directional LER -- GOME-2 LER v3.0.....	5
3.1 New features of DLER.....	5
3.2 Implementation of DLER.....	7
3.3 Improvements in FRESCO+ v2 due to the DLER.....	7
4 Summaries.....	18

Table of Figures

Figure 1 Simulated GOME-2C reflectance spectrum at the GOME-2C nominal wavelength grid. The reflectances at the FRESCO wavelength grid are marked with blue symbols.....	5
Figure 2 An example of (a) surface minimum DLER over Amazonia (vegetation) and (b) mode DLER over Sahara deserts for March. The circles show the retrieved surface LER for the five viewing angle containers. The associated VZA of the container contents is plotted on the horizontal axis. (Figures are provided by G. L. Tilstra.).....	6
Figure 3 GOME-2 Mode LER at 772 nm version 2 (left) and 3 (right) for March. (Figures are provided by L.G. Tilstra.).....	6
Figure 4 MODIS Terra corrected reflectance true color image on 15 April. (image from NASA worldview, https://worldview.earthdata.nasa.gov/).....	8
Figure 5 FRESCO cloud fraction retrieved using LER for one GOME-2A orbit on 15 April 2010.	9
Figure 6 FRESCO cloud fraction retrieved using DLER for one GOME-2A orbit on 15 April 2010.....	9
Figure 7 FRESCO cloud pressure retrieved using LER for one GOME-2A orbit on 15 April 2010.....	10
Figure 8 FRESCO cloud pressure retrieved using DLER for one GOME-2A orbit on 15 April 2010.....	10
Figure 9 Global map of averaged surface albedo at 15 FRESCO wavelengths using DLER over land for GOME-2A data in April 2010. Snow/ice pixels are excluded.....	12
Figure 10 Global map of surface albedo difference (averaged surface albedo DLER-LER) over land for GOME-2A data in April 2010. Snow/ice pixels are excluded.....	12
Figure 11 Global map of cloud fraction retrieved using DLER over land for GOME-2A data in April 2010.....	13

Figure 12 Global map of cloud fraction difference (DLER-LER) over land for GOME-2A data in April 2010.....13

Figure 13 Global map of cloud pressure retrieved using DLER over land for GOME-2A data in April 2010, unit: hPa.....14

Figure 14 Global map of cloud pressure difference (DLER-LER) over land for GOME-2A data in April 2010. Unit: hPa. Snow/ice pixels are excluded.....14

Figure 15 Averaged surface albedo over 15 FRESCO wavelengths over land for GOME-2A data in April 2010, left: DLER, right: LER.....15

Figure 16 Cloud fraction as a function of cross track index over land for GOME-2A data in April 2010, left: DLER, right: LER.....15

Figure 17 Cloud pressure as a function of cross track index over land for GOME-2A data in April 2010, left: DLER, right: LER, unit: hPa.....16

Figure 18 Chi-squared as a function of cross track index overland for GOME-2A data in April 2010, left: DLER, right: LER.....16

Figure 19 Global map of averaged surface albedo at 15 FRESCO wavelengths using DLER over ocean for GOME-2A data in April 2010. Snow/ice pixels are excluded.....17

Figure 20 Global map of surface albedo difference (averaged surface albedo DLER-LER) over ocean for GOME-2A data in April 2010. Snow/ice pixels are excluded.....17



1 Introduction

This is the report of WP1 of the project, *FRESCO+ version 2 for GOME-2 Metop-C processing*. The report includes a short describe the FRESCO+ v2 look-up tables (LUT) for GOME-2C and the instruction of using DLER in FRESCO+ v2.

2 FRESCO+ v2 LUT for GOME-2C

FRESCO+ v2 retrieves effective cloud fraction and cloud pressure using the oxygen A-band absorption and taking into account single Rayleigh scattering (Wang et al., 2008). The FRESCO cloud retrieval algorithm is based on look-up tables (LUTs). The transmissions and reflectances of the O₂ A band are simulated at high spectral resolution and convolved with the GOME-2 instrument slit function. Then the transmissions and reflectances at 15 selected wavelengths of the GOME-2 instrument are stored in the look-up tables. The LUTs are instrument-specific, because the slit function and the wavelength sampling of the spectrum are different for every GOME-2 instrument.

The FRESCO+ v2 algorithm has been implemented in the GOME-2 PPF through the EUMETSAT contract EUM/CO/16/4600001774/RL in 2017 (Wang et al., 2017). The implementation has led to improved performance and data quality in the GOME-2A and -B PPF. The FRESCO cloud products are an important input for several L2 algorithms.

The slit function of GOME-2C used in the LUTs are taken from slit-function key data version 1.6 (Siddans et al., 2018, filename SFS_SLIT_MAIN.201_3N_1_0.v1.6). The O₂ line parameters in HITRAN 2008 database are used to calculate the O₂ absorption at 0.001 nm equal-distant grid. The 15 wavelengths between 589-590, 760-761, 765-766 nm are selected from the nominal wavelength grid in the key data. Figure 1 shows the simulated O₂ A band spectra using GOME-2C slit function at 760 nm. The full width half maximum of the GOME-2C slit function is very similar to that of GOME-2A/B. As shown in Fig. 1, the spectrum looks quite smooth. The LUTs have the same format as the LUTs for GOME-2A/B. The settings used the in the transmission tool are provided in the appendix and also in the headlines of the LUTs.

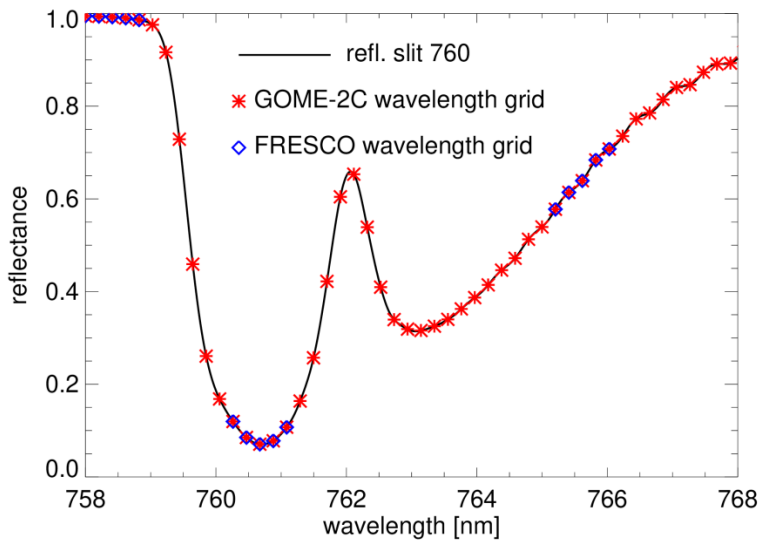


Figure 1 Simulated GOME-2C reflectance spectrum at the GOME-2C nominal wavelength grid. The reflectances at the FRESCO wavelength grid are marked with blue symbols.

3 Directional LER -- GOME-2 LER v3.0

3.1 New features of DLER

At the time of the implementation of FRESCO+ v2, the GOME-2 LER database v2.1 was the most suitable surface albedo database available, because it covers the relevant spectral bands and is derived from GOME-2 data itself (Tilstra et al., 2017). However, this database does not include the view-angle dependence of the surface reflection. This dependence is especially important for land surfaces, and is part of the so-called BRDF. Recently the a directional LER is developed to include view-angle dependence in the LER surface albedo database v3.0 (Tilstra et al., 2018). The surface DLER can now be calculated per month and wavelength band as a function of the latitude, longitude, and viewing zenith angle (VZA). The database is derived from a combination of GOME-2A and -B data (2007-2018) and has an intrinsic resolution of 1.0 x 1.0 degrees, increased to 0.25 x 0.25 degrees at the coastlines and for certain specific regions such as snow covered mountain ranges. This is achieved using dynamical gridding. The database grid itself has a 0.25 x 0.25 degrees resolution and an iterative/repeated bilinear interpolation scheme was used to get to this resolution globally (Tilstra et al., 2018).

Figure 2 shows the DLER over vegetation and deserts. As shown in Fig. 2, the surface albedos at 758 and 772 nm, which are used in FRESCO+ retrievals, have a strong VZA dependence over vegetation. The directional components of the DLER are not available over ocean.



Based on some preliminary analysis, we find that using the DLER database improves the quality of the retrieved effective cloud fraction and cloud pressure over land. In the current GOME-2 cloud products, the effective cloud fractions at the west side of an orbit are often too high over land, because of the missing angular dependence of the surface albedo. The DLER has to be implemented for all GOME-2 instruments for the sake of consistency of the GOME-2 cloud products.

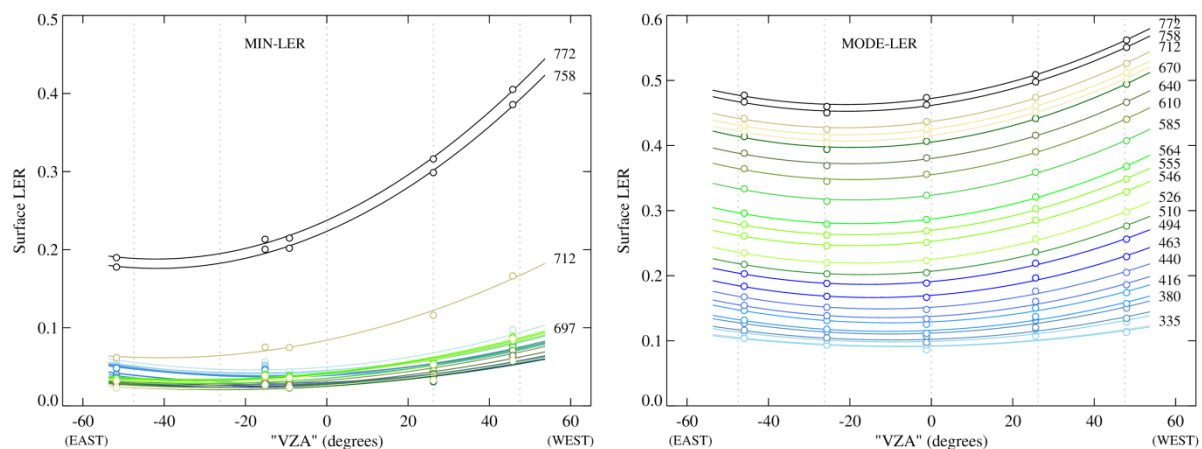


Figure 2 An example of (a) surface minimum DLER over Amazonia (vegetation) and (b) mode DLER over Sahara deserts for March. The circles show the retrieved surface LER for the five viewing angle containers. The associated VZA of the container contents is plotted on the horizontal axis. (Figures are provided by G. L. Tilstra.)

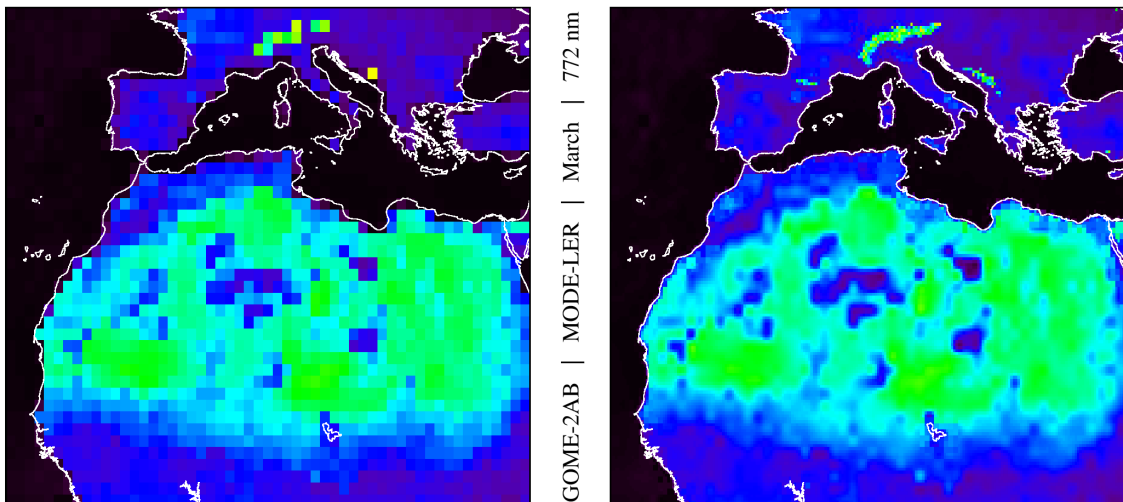


Figure 3 GOME-2 Mode LER at 772 nm version 2 (left) and 3 (right) for March. (Figures are provided by L.G. Tilstra.)



3.2 Implementation of DLER

The LER v3.0 is provided in HDF5 format. The fields `Min_Mode_LER`, `Minimum_LER`, and `Mode_LER` are the LER values without the VZA dependence. The newly introduced data sets `Polynomial_coefficients_min_mode_LER`, `Polynomial_coefficients_minimum_LER`, `Polynomial_coefficients_mode_LER` are the polynomial coefficients to describe the VZA dependence of the corresponding LER.

The recipe for the implementation of the DLER in FRESCO+ v2 is as follows:

- (1) Read in the normal "Min_Mode_LER" field for 758 and 772 nm.
- (2) Read in the new "Polynomial_coefficients_min_mode_LER" field for 758 and 772 nm.
- (3) Take the VZA of GOME-2 observation, and make it negative if the observations is from the eastern side of the orbit swath (that is, for `IndexInScan` = 1--12 in the forward scan and for `IndexInScan` = 29--32 in the back scan).
- (4) Calculate the directional surface LER (A_{DLER}) according to Eq. 1:

$$A_{DLER} = A_{LER} + c_0 + c_1\theta + c_2\theta^2, \quad (1)$$

where A_{LER} is the normal `min_mode_LER` obtain in step (1); c_0 , c_1 , c_2 are polynomial coefficients for `min_mode_LER` obtained in step (2); θ is the VZA*, unit degree, calculated in step (3). The polynomial coefficients define parabolic corrections to the non-directional surface LER. In step (4), the corrections use VZA* (the VZA that was made negative at the Eastern side of the swath).

DLER over the ocean is not provided, and the Polynomial coefficients are zeros. Therefore, do not expect any differences over the oceans between the LER and DLER.

3.3 Improvements in FRESCO+ v2 due to the DLER

After implemented the DLER in FRESCO+ v2, we have reprocessed GOME-2A data to check the improvements. The comparison of one month of GOME-2A data in April 2010 with DLER and with normal LER is shown in this report. The only difference between this two data set is the surface albedo. Figure 4 shows the MODIS Terra image over South America on 15 April 2010. The overpass time of MODIS Terra is close to the overpass time of GOME-2A but not the same orbit. In the MODIS image, there are some cloud-free areas over vegetation. We compared FRESCO cloud products using LER and DLER for this region because the DLER has large VZA dependence over vegetation. And the DLER or LER has large impact on the FRESCO cloud product for almost cloud-free scenes. Figures 5 and 6 show the FRESCO cloud fraction retrieved using LER and DLER, respectively. Over the cloud-free regions, the cloud fraction with LER



shows some small values (~ 0.2) at the west part of the orbit, while the cloud fraction with DLER is very close to 0. Over ocean, Figs. 5 and 6 are the same. Figures 7 and 8 show the cloud pressure retrieved using LER and DLER. At the west part of the orbit, the cloud pressure retrieved using DLER is lower than the cloud pressure retrieved using LER.

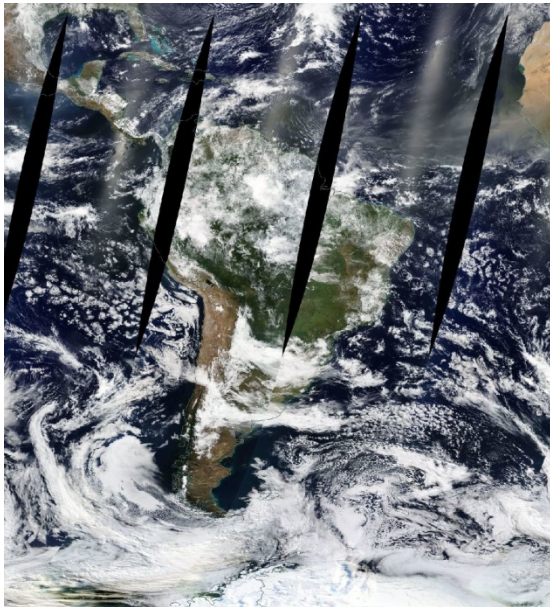


Figure 4 MODIS Terra corrected reflectance true color image on 15 April. (image from NASA worldview, <https://worldview.earthdata.nasa.gov/>)

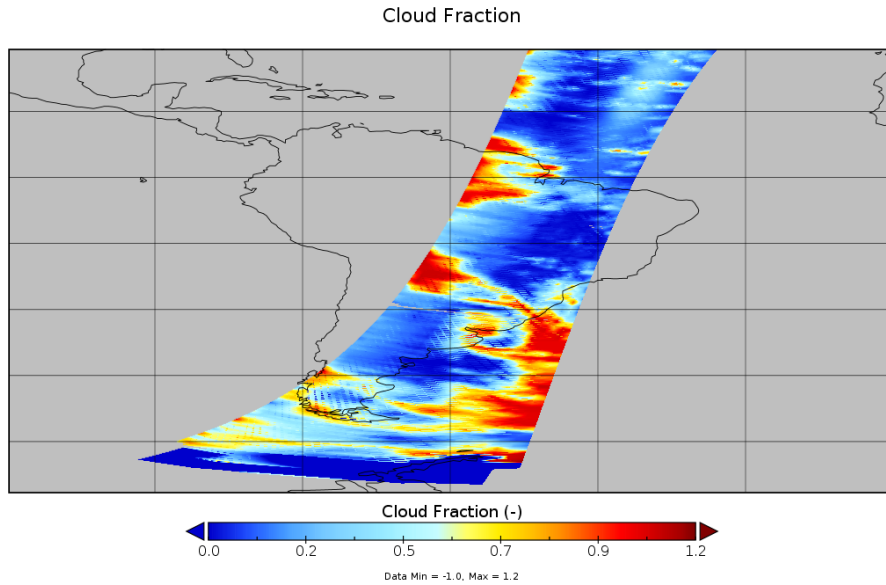


Figure 5 FRESCO cloud fraction retrieved using LER for one GOME-2A orbit on 15 April 2010.

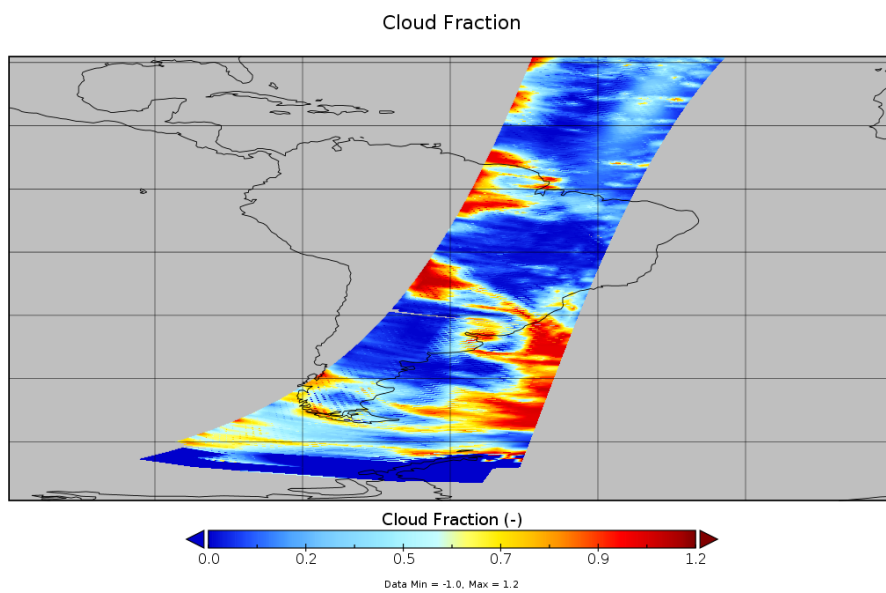


Figure 6 FRESCO cloud fraction retrieved using DLER for one GOME-2A orbit on 15 April 2010.

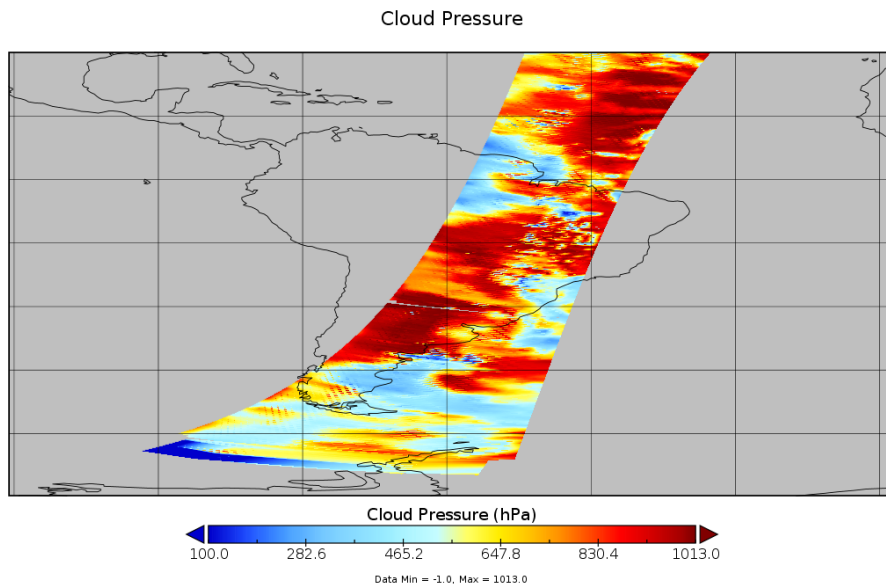


Figure 7 FRESCO cloud pressure retrieved using LER for one GOME-2A orbit on 15 April 2010.

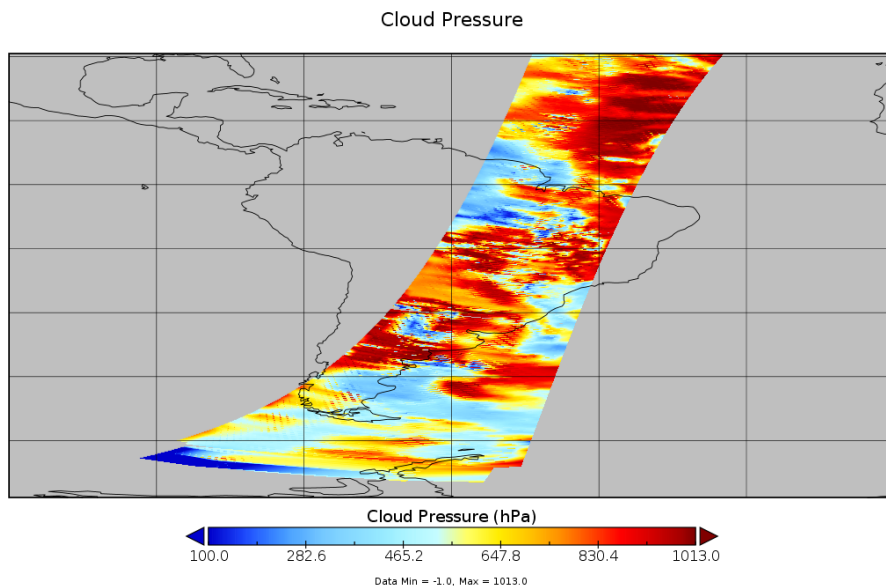


Figure 8 FRESCO cloud pressure retrieved using DLER for one GOME-2A orbit on 15 April 2010.

In order to get more statistics, we have analysed the full month of GOME-2A data retrieved using LER and with DLER in April 2010. The data over land and ocean are separated in the comparison because there is no difference in the data over ocean. Data having surface height of 0 km and surface albedo smaller than 0.05 are classified as over ocean. Some pixels close to



coastlines and islands may not be classified as land/ocean correctly. Figure 9 shows the averaged surface albedo in April 2010 in FRESCO output using DLER. The difference between the surface albedo of DLER and LER is shown in Fig. 10. The DLER shows some high values than the LER because the DLER at the west side of an orbit is larger than the LER at the west side of an orbit.

Figures 11 and 12 show the cloud fraction using DLER and the differences for April 2010, respectively. In the monthly averaged cloud fraction images, it is not easy to see the VZA dependence of the cloud fraction because at any particular location, the cloud fractions are measured at different VZA in a month. The monthly mean cloud fraction is an average of cloud fractions from different VZA. However, it can be seen that the monthly mean cloud fraction with DLER is mostly smaller than the monthly mean cloud fraction with LER over vegetation. The DLER has also impacts on cloud pressure. As shown in Figs. 13 and 14, the cloud pressures retrieved using DLER are lower than the cloud pressure retrieved using LER, especially over vegetation.

The cross track surface albedos of DLER and LER are shown in Figs. 15. The DLER has larger surface albedo for the west pixels (pixel No. 13-24) than for the east pixels (pixel no. 1-12). For the LER, the surface albedos are the same for the cross track pixel position and the values are close to the DLER of the east pixels. The cross track cloud fraction using DLER seems symmetric while the cloud fraction using LER has a positive bias at the west pixels (see Fig. 16). We expect that the monthly mean global mean cloud fraction does not depend on the cross track position of the pixel. The slightly larger cloud fraction at the two sides of swath (east and west side) is due to the assumption of Lambertian clouds in the FRESCO algorithm. Figure 17 shows the monthly mean cross track cloud pressure for April 2010. Similar to the cloud fraction, the cloud pressure retrieved using DLER is also more realistic than the cloud pressure retrieved using LER. As shown in Fig. 18, the fit of measured and simulated spectra is also improved when using DLER especially for the west pixels.

Surface albedo of the DLER and the difference between DLER and LER over ocean are shown in Figs. 19 and 20, respectively. This is used to check if the DLER is implemented correctly. There is almost no difference between the DLER and LER over ocean. There are a few small differences at the high latitudes, which might be due to the snow/ice pixels.

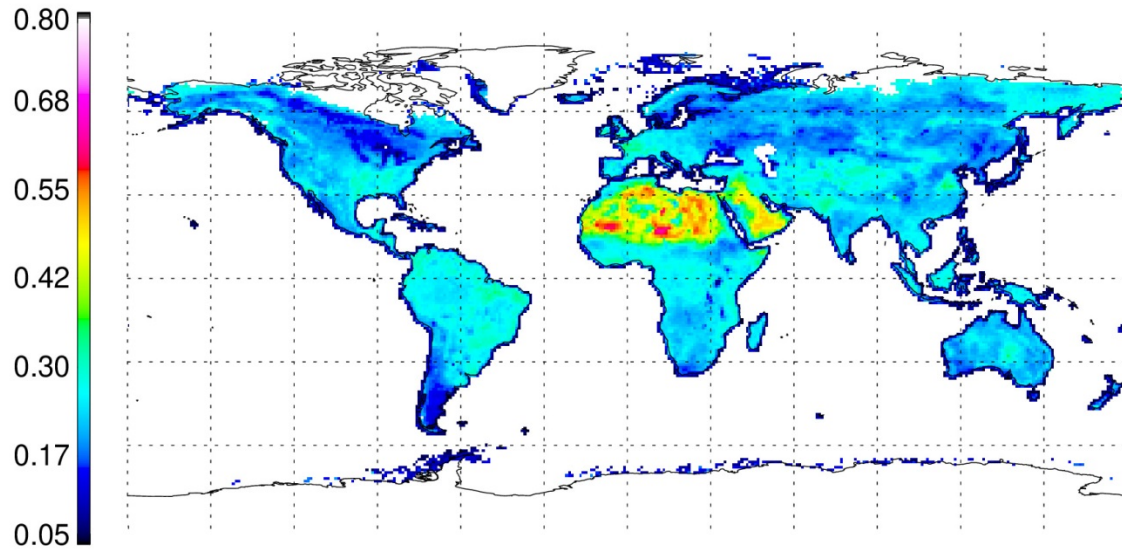


Figure 9 Global map of averaged surface albedo at 15 FRESCO wavelengths using DLER over land for GOME-2A data in April 2010. Snow/ice pixels are excluded.

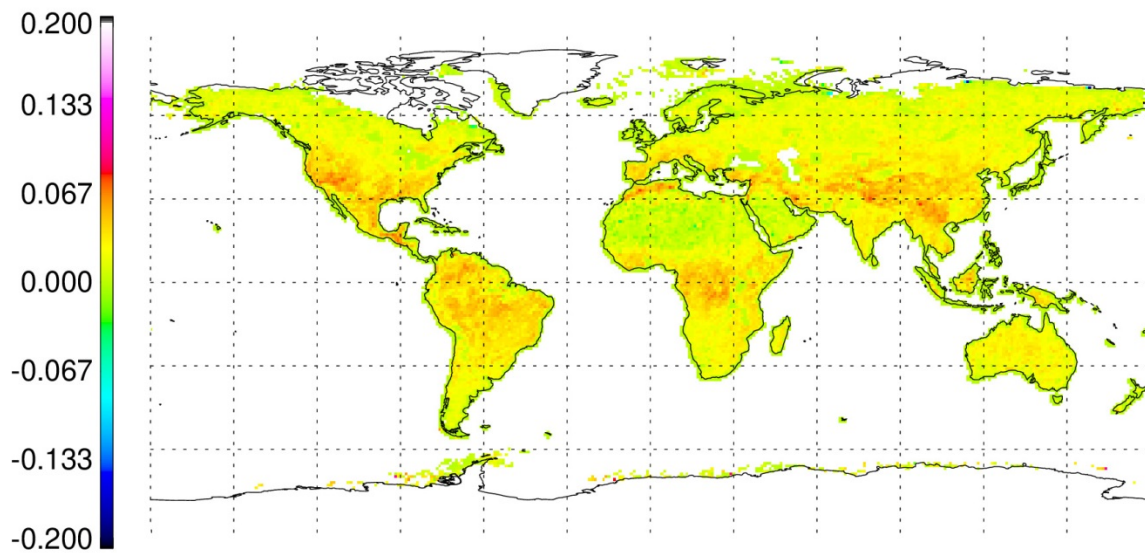


Figure 10 Global map of surface albedo difference (averaged surface albedo DLER-LER) over land for GOME-2A data in April 2010. Snow/ice pixels are excluded.

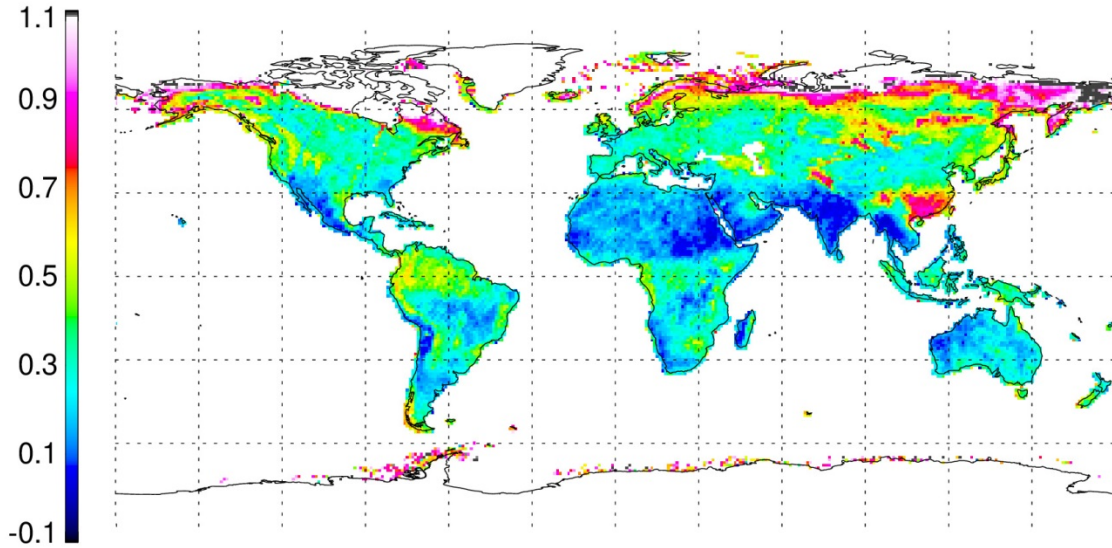


Figure 11 Global map of cloud fraction retrieved using DLER over land for GOME-2A data in April 2010.

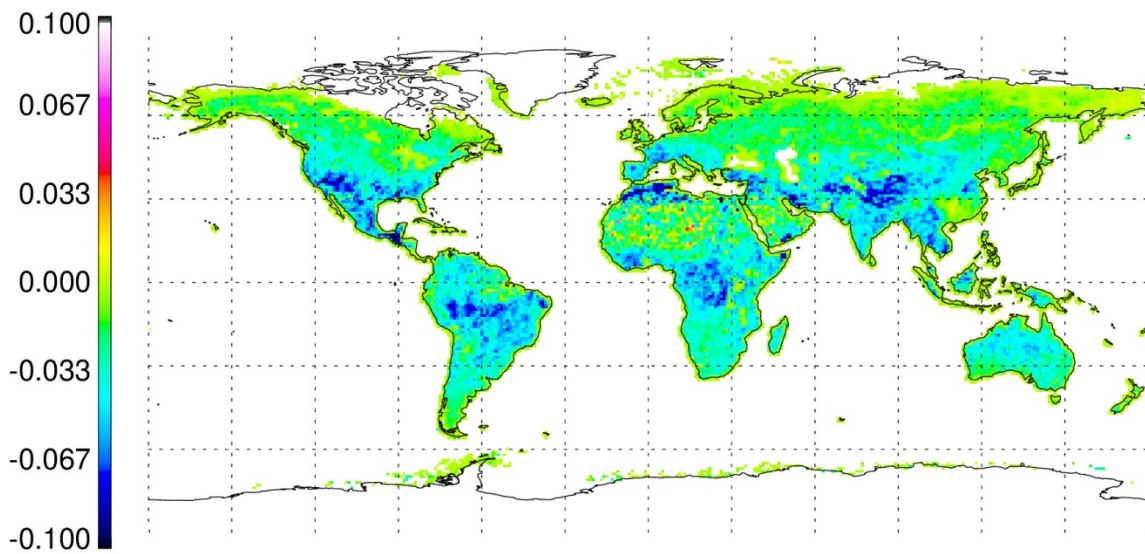


Figure 12 Global map of cloud fraction difference (DLER-LER) over land for GOME-2A data in April 2010.

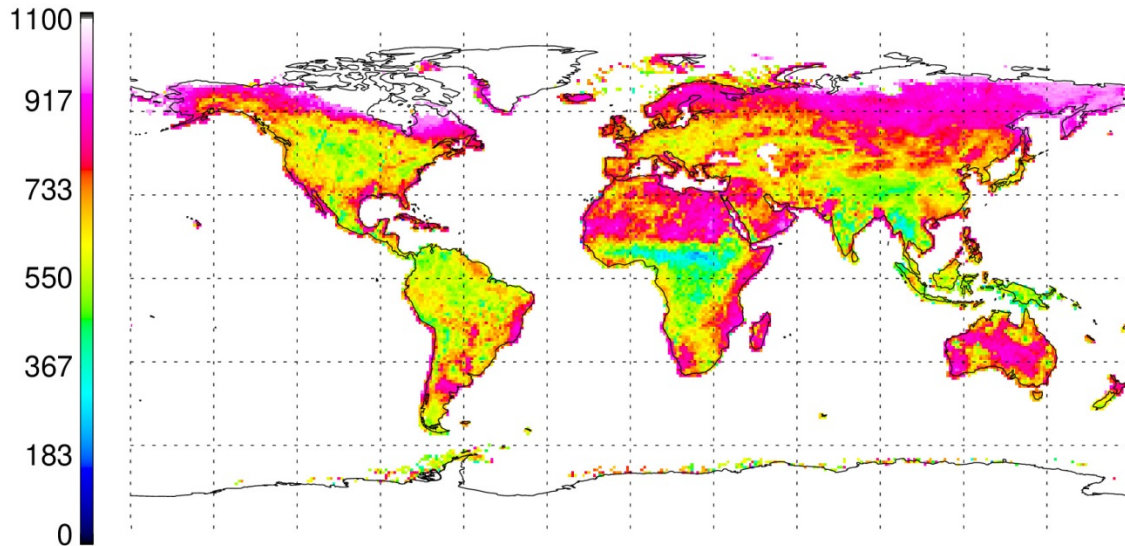


Figure 13 Global map of cloud pressure retrieved using DLER over land for GOME-2A data in April 2010, unit: hPa.

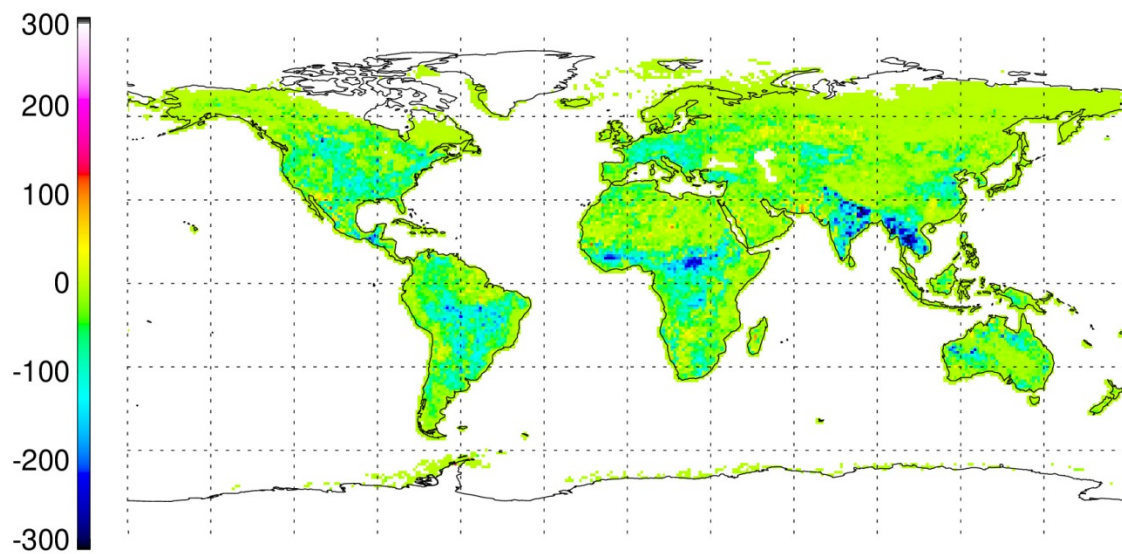


Figure 14 Global map of cloud pressure difference (DLER-LER) over land for GOME-2A data in April 2010. Unit: hPa. Snow/ice pixels are excluded.

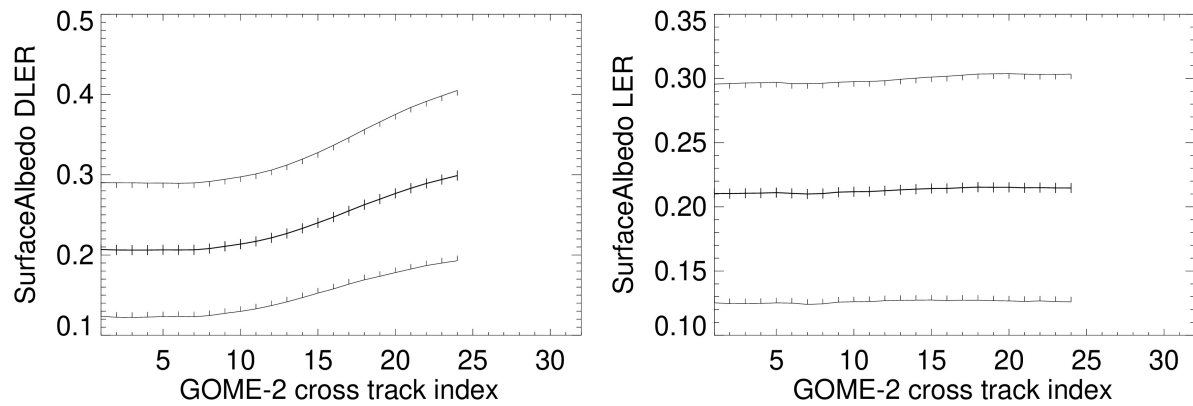


Figure 15 Averaged surface albedo over 15 FRESCO wavelengths over land for GOME-2A data in April 2010, left: DLER, right: LER.

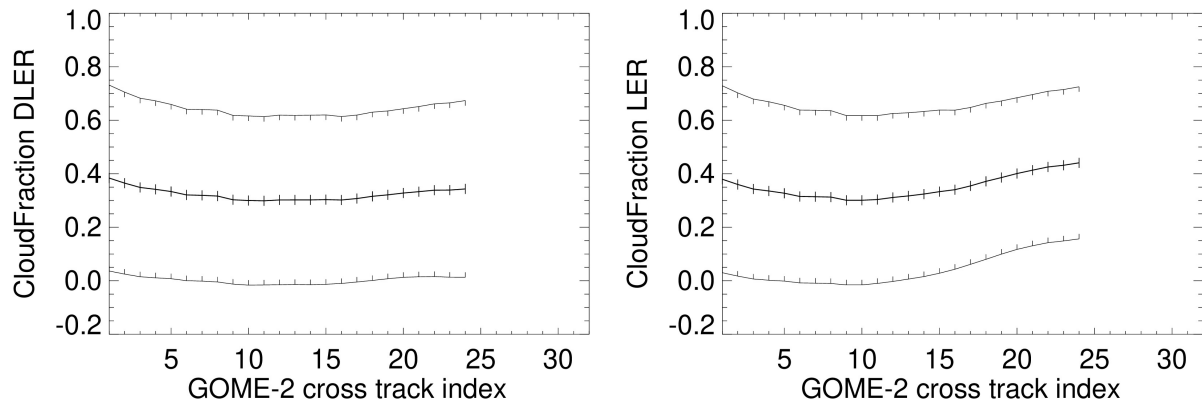


Figure 16 Cloud fraction as a function of cross track index over land for GOME-2A data in April 2010, left: DLER, right: LER.

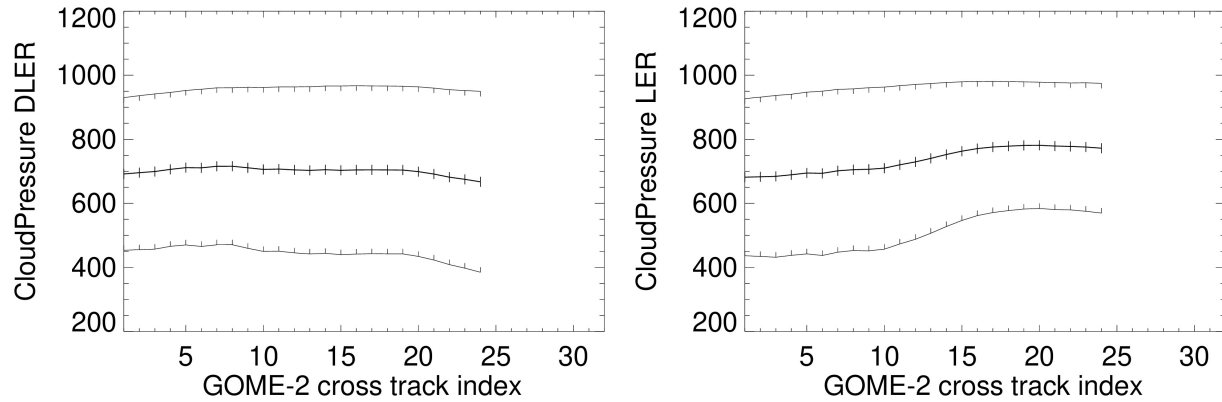


Figure 17 Cloud pressure as a function of cross track index over land for GOME-2A data in April 2010, left: DLER, right: LER, unit: hPa.

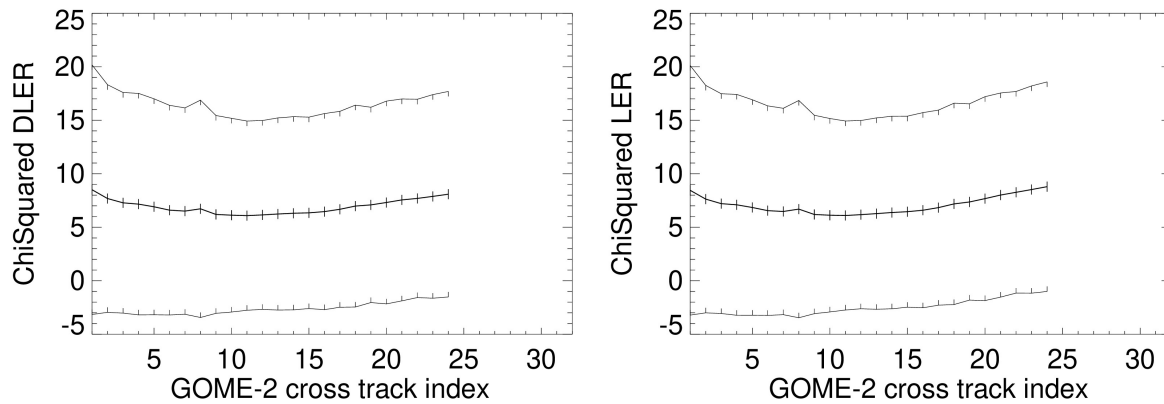


Figure 18 Chi-squared as a function of cross track index overlant for GOME-2A data in April 2010, left: DLER, right: LER.

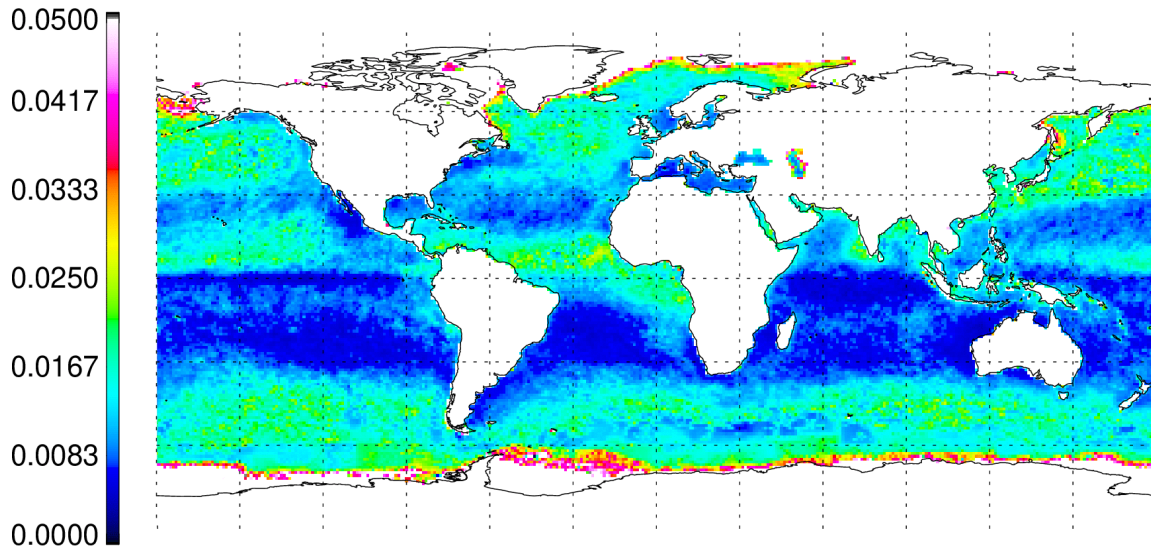


Figure 19 Global map of averaged surface albedo at 15 FRESCO wavelengths using DLER over ocean for GOME-2A data in April 2010. Snow/ice pixels are excluded.

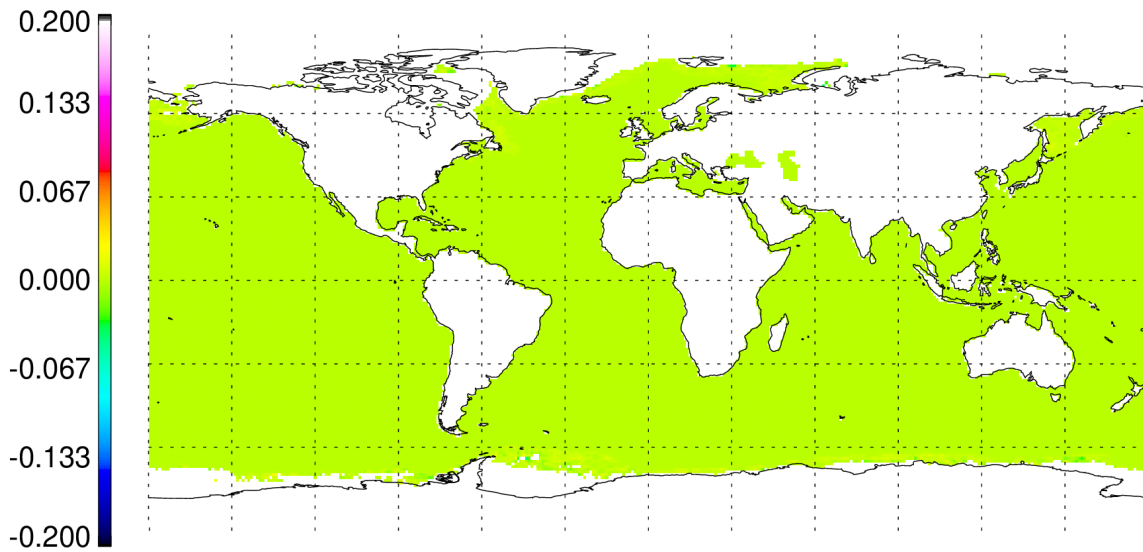


Figure 20 Global map of surface albedo difference (averaged surface albedo DLER-LER) over ocean for GOME-2A data in April 2010. Snow/ice pixels are excluded.



4 Summaries

The LUTs for GOME-2C has been generated using HITRAN 2008 using the GOME-2C ISRF at the nominal wavelength grid. The LER v3.0 including DLER and other improvements over deserts and coastlines has been implemented in KNMI FRESCO+ v2 (or FRESCO v8). Based on the comparisons of FRESCO with DLER and with LER, we found that FRESCO using LER v3.0 (DLER) gives the best results until now. The cross track bias in cloud fraction and cloud pressure have been removed.

Reference

Siddans et al. Analysis of GOME-2 Slit function Measurements: Final Report Eumetsat Contract No. EUM/CO/04/1298/RM, DATE: 10-07-2018.

Tilstra, L. G., O.N.E. Tuinder, P. Wang, and P. Stammes, Surface reflectivity climatologies from UV to NIR determined from Earth observations by GOME-2 and SCIAMACHY, J. Geophys. Res. Atmos. 122, doi:10.1002/2016JD025940, 2017.
(http://www.temis.nl/surface/gome2_ler.html)

Tilstra, L.G., O.N.E. Tuinder, P. Stammes, 2018, Algorithm Theoretical Basis Document, GOME-2 surface LER product, SAF/AC/KNMI/ATBD/003, issue 3.0, 26 September, 2018.

Tilstra, L.G., O.N.E. Tuinder, P. Stammes, 2018, Product User Manual, GOME-2 surface LER product, SAF/AC/KNMI/PUM/004, issue 3.0, 26 September, 2018.

Wang, P., P. Stammes, R. van der A, G. Pinardi en M. van Roozendaal, FRESCO+: an improved O2 A-band cloud retrieval algorithm for tropospheric trace gas retrievals, *Atm. Chem. Phys.*, 2008, 8, 9697-9729.

Wang, P., O.N.E. Tuinder, P. Stammes, 2017, Upgrade of FRESCO+ to version 2 in the GOME-2 Product Processing Facility, Final report, 11 August 2017, EUM/CO/16/4600001774/RL.



Settings for generation of the look-up table

!*****FRESCO transmission program input file*****

FRESCO or FRESCO+ transmission program, 1: FRESCO, 2: FRESCO+
2

! This optional determine the transmission database format.

Transmission database for GOME-2 or SCIAMACHY, 1: GOME-2, 2: GOME/SCIAMACHY
1

Directory for all input files

./

! HITRAN parameters

Molecule number in HITRAN database (igas)

7 ! O2=7, H2O=1, CO2=2, NH3=11 ...

! If using any other molecule than O2, H2O, CO2, or NH3,

! the mass of molecule and mixing ratio profile must be given as input.

! The HITRAN database file should also be given for igas.

! The mixing ratio of the molecule (igas) should be defined in the atmospheric

! profile file in column 9. Thereto replace CIO profile to 'igas' profile,

! unit [ppmv].

Mass of molecule (not used for O2, H2O,CO2, NH3)

-1.0 ! m_mol is molecular mass in g/mol

HITRAN database version format (2001: for version 2001,2004: for version 2004 and later)

2004

HITRAN filename for selected molecule (igas)

'07_hit09.par'

High resolution wavelength grid type: 1) equidistant, 2) shifted, 3) external file

3

Start wavelength of high resolution wavelength grid [nm]

756.0



End wavelength of high resolution wavelength grid [nm]
769.5

Wavelength step of high resolution wavelength grid [nm]
0.001

External wavelength grid file (only used when wavelength grid type is 3).
'hitran2009_wavelgrid_gome2ab_res1pm_short.dat'

Wavelength range for Voigt line profile (range = -dwav, +dwav) [nm]
10.0 ! dwav

! Geometric parameters

Start Solar zenith angle [degree]
0.0

End Solar zenith angle [degree]
90.0

Solar zenith angle step [degree]
1.0

Start viewing zenith angle [degree]
0.0

End viewing zenith angle [degree]
70.0

Viewing zenith angle step [degree]
1.0

Atmospheric profile file
'mls_afgl.dat2'

! Instrumental parameters

Name of file with wavelength grid for convolution
'wavgome2c_o2a.dat.v0'

Number of header lines in wavelength grid file



28 15 ! number of lines in header and number of wavelengths

Slit function type, 1: tabulated, 2: analytic

1

Slit function filename (only used for tabulated SF)

'gome2c_sf201_wav15_v0.dat'

! If use 15 slit function, the slit function wavelength grid should be the

! same as the wavelength grid for the convolution.

! If the wavelength difference is great than or equal 0.1 nm the program will stop.

! If the wavelength difference is little than 0.1 nm but not 0

! the program print a warning message on the screen.

Which slit function to be used (only used for tabulated SF)

-999 ! -999: use all slit functions; 1-15: use slit function No. #

Number of header lines in slit function file (only used for tabulated SF)

1 ! number of lines in header

The slit function wavelength range (-delta, +delta) [nm]

1.31

! Output options

Directory for all output files

'./'

! If output filename is set to 'DEFAULT' it use the standard output filenames:

! polycoef.dat, log.dat, and tsim.dat.

! tau.dat trs.dat for high spectral resolution optical thickness and

! transmission.

! If user defined filename, the output files are filename.polycoef.dat,

! filename.log.dat, and filename.tsim.dat.

! filename.tau.dat, filename.trs.dat for high spectral resolution

! optical thickness and transmission.

Output filename, DEFAULT or user defined filename

'gome2c.hit9.grid3'



!
! Additional output for high spectral resolution total optical thickness
! and total transmission at certain SZA, VZA and layer.
!
High resolution total optical thickness (.true. or .false.)
.true.

High resolution transmission (.true. or .false.)
.true.

SZA and VZA for transmission output
60.0, 0.0

The output level 1-31. 1: 0km, 31: 15 km for high resolution transmission.
17

! The transmission output includes two levels.
! The level at the surface (layer 1) is always in the output,
! so this cloud level here is to choose another level above the surface.
! FRESCO use equidistant altitude grid, every layer is 0.5 km.

! End of input file